


High-Mass MALDI-MS Analysis for the Investigation of Protein Encapsulation within an Engineered Capsid Forming Protein

Journal Article**Author(s):**

Root, Katharina; Frey, Raphael; Hilvert, Donald; [Zenobi, Renato](#) 

Publication date:

2017-10

Permanent link:

<https://doi.org/10.3929/ethz-b-000185233>

Rights / license:

[In Copyright - Non-Commercial Use Permitted](#)

Originally published in:

Helvetica Chimica Acta 100(10), <https://doi.org/10.1002/hlca.201700166>

Funding acknowledgement:

159929 - Soft ionization mass spectrometry for studying noncovalent interactions (SNF)

High-Mass MALDI-MS Analysis for the Investigation of Protein Encapsulation within an Engineered Capsid Forming Protein

Katharina Root, Raphael Frey, Donald Hilvert, and Renato Zenobi*

Department of Chemistry and Applied Biosciences, ETH Zurich, CH-8093, Zurich, Switzerland

ABSTRACT

Chemical cross-linking combined with MALDI-MS was applied to structural analysis of a protein nanocontainer. Specifically, an engineered variant of lumazine synthase from *Aquifex aeolicus* (AaLS-13) was investigated that self-assembles into a capsid-like structure and is known to encapsulate other proteins by Coulombic attraction. Two complementary soft ionization techniques, MALDI-MS and native ESI-MS, were utilized to map the subunit stoichiometry of the high molecular weight capsid. In accordance with the previously reported cryo-electron microscopy structure of this protein container, only pentameric subunits were detected. This study highlights the possibility to map subunit stoichiometry via chemical cross-linking with glutaraldehyde followed by MALDI-MS. The same approach was used to study protein-protein interactions during encapsulation of GFP(+36) by the AaLS-13 capsid. Heterocomplexes between GFP(+36) and AaLS-13 multimers were not observed when mixed at maximal loading capacity (AaLS-13 monomer:GFP(+36) 4:1). This is in agreement with the known fast encapsulation of GFP(+36) by the protein capsid, which essentially removes any free GFP(+36) from the solution. Exceeding the maximal loading capacity by addition of excess GFP(+36) results in aggregation.

Keywords: Capsids • icosahedron • Native-ESI MS • MALDI-MS • chemical cross-linking MS • noncovalent complexes

This article has been accepted for publication and undergone full peer review but has not been through the copyediting, typesetting, pagination and proofreading process, which may lead to differences between this version and the Version of Record. Please cite this article as doi: 10.1002/hlca.201700166

This article is protected by copyright. All rights reserved.

INTRODUCTION

Mass spectrometry (MS) has evolved into a powerful tool for structural and functional analysis of protein complexes.^[1, 2] Native ESI-MS in particular has been established as a promising analytical technique to study biomolecular complexes. Another soft ionization technique is MALDI-MS, which is much less common to study non-covalent associates, predominantly because MALDI can induce complex dissociation either during sample preparation or the ionization process. However, specific methodologies have been developed to overcome issues with complex dissociation in both the desorption/ionization process and during incorporation of non-covalent complexes into matrix crystals^[3, 4], allowing analysis of biomolecular complexes by MALDI. Compared to native ESI, analysis of such samples by MALDI also has some obvious advantages, in particular the ability to work in the presence of fairly high concentrations of salts (up to the mM range), buffers and detergents.^[4, 5]

The investigation of proteinaceous nanocontainers, as in the example shown here, with molecular weights in the MDa range is nevertheless challenging due to the limited mass range of many instruments and the low mass resolution at very high m/z . Moreover, bringing such high molecular weight proteins into the gas phase may result in changes to their quaternary or tertiary structures. Incomplete desolvation is an additional problem, particularly for capsids in the megadalton range, resulting in poor quality signals.^[6, 7] Nevertheless, the analysis of high-molecular weight capsids by mass spectrometry is very attractive, since it allows determination of the molecular weight, as well as stoichiometry and composition.^[7] High-molecular-weight capsids have been successfully studied with MS by several research groups, using almost exclusively ESI.^[1, 2, 7-9, 10, 11] Jarrold and co-workers have developed a charge detection scheme where the m/z and z of individual ions are measured concurrently, thereby allowing direct determination of the mass of each ion.^[8] They have, for example resolved the heterogeneity of adeno-associated viruses (AAVs) in the 4 - 5 MDa mass range.^[8] The group of Bier is one of the very few employing MALDI-MS to study large clusters and capsids. Using superconducting tunneling junction cryodetection, they were able to determine the masses of intact horse spleen (HS) apoferritin, HS-holoferitin, and the HS-holoferitin dimer to be ~505 kDa, ~835 kDa, and ~1.63 MDa, respectively.^[12] More insightful to understand capsid assembly, however, are studies where the subunit stoichiometry of such capsids is probed: using ESI-MS, Tito *et al.* were able to detect and confirm the stoichiometry of the bacteriophage MS2 with a molecular weight of >2 MDa^[10], while Heck and co-workers have successfully employed native ESI-MS for the investigation and characterization of intact high molecular weight viruses and viral capsids in the gas phase.^[1, 11]

Molecular containers constructed from self-assembling proteins enable highly specialized biological functions. Proteins capable of forming regular hollow shell-like structures have generated interest due to their potential applications as containers for drug delivery and as nanoreactors for improved catalytic control.^[13, 14-16] In nature, encapsulation often takes place by the recognition of the cargo through noncovalent interactions, which can be exploited for the loading of a guest molecule of interest such as enzymes and drug molecules.^[15-17] A frequently used protein nanocage for diverse biotechnological applications is the iron-storing protein ferritin.^[18] The potential of this protein cage was recognized when ferritin was produced without its mineralized iron core, viz. apo-ferritin, which could be loaded with various other metals.^[19] Further examples of protein cages with applications in drug delivery and catalysis are viral capsids, as well as bacterial microcompartments, proteinaceous organelles that sequester multiple enzymes from a metabolic pathway thereby increasing the specificity, reaction control and catalytic performance.^[20]

Here, we report the investigation of an encapsulation system based on an engineered variant of the capsid-forming protein lumazine synthase from *Aquifex aeolicus*, AaLS-13.^[14, 21] The luminal surface of the protein shell is highly negatively charged, which enables host-guest interactions with positively charged cargo molecules such as a supercharged variant of green fluorescent protein GFP(+36) and fusions thereof.^[15, 22-24] In order to create a highly positively charged variant of GFP, 29 solvent exposed positions were identified in the crystal structure and mutated to Lys and Arg residues, yielding a variant with a theoretical net charge of +36.^[22] Recently, the structure of the AaLS-13 capsid was solved using cryo-electron microscopy.^[25] The ~6 MDa assembly is constructed from 72 pentameric subunits that adopt an unprecedented icosahedrally symmetric structure, with large keyhole-shaped pores that allow rapid passage of positively charged protein cargo.^[25, 26] Using this structurally well-characterized capsid as an example, we show that crosslinking combined with high-mass MALDI and native ESI mass spectrometry can be used as complementary tools to rapidly gain information about subunit composition of a protein container as well as the process of cargo encapsulation.

RESULTS AND DISCUSSION

Determination of the Subunit Stoichiometry. We first show that chemical cross-linking combined with high-mass MALDI-MS can be used as a complementary analytical technique to provide rapid insight into the structure of AaLS-13 capsids. Although MALDI is a soft ionization technique, it is less gentle

than ESI, and noncovalent interactions are often disrupted either during MALDI sample preparation or ionization processes. Therefore, chemical cross-linking in native solution prior to analysis is advantageous for the stabilization of noncovalent complexes. We used glutaraldehyde (GA, 1% concentration), a well known and efficient cross-linking reagent that mainly targets primary amine groups, with additional reactivity towards other nucleophiles including guanidines, secondary amines, hydroxyl groups and thiols.^[27] GA was employed here for chemical stabilization of the capsid and any subunits present in solution. In order to achieve successful cross-linking, the protein structure, and in particular the distances between free amines, are of great importance. These should be solvent accessible as well as close to each other, within reach of the cross-linker. The experiments were carried out using optimized buffer conditions (50mM NaP, 200mM NaCl, 5mM EDTA, I=350 mM), found to be a good compromise between too low salt concentrations (favoring capsid cargo complex formation, but potentially leading to undesired precipitation) and too high salt concentration (to avoid precipitation, but resulting in lower encapsulation yields).^[26] Parameters including pH, ionic strength, GA concentration and temperature were carefully optimized and monitored over time. All experiments were carried out at room temperature because AaLS-13 capsid showed precipitation upon cooling.

We first applied high-mass MALDI-MS to study the subunit composition. The experiments were carried out after having confirmed the presence of pentamer and capsid fractions using SEC (data not shown). Figure 1a) (black trace) shows AaLS-13 prior to cross-linking. The dominant peak at $m/z = 17,700$ can be attributed to the monomer (theoretical MW = 17,684) since the quaternary structure is not maintained in the absence of a stabilizing cross-linker. The peak at $m/z = 35,600$ is a dimer, typical for unspecific clustering in the MALDI plume. Applying chemical cross-linking prior to analysis with high mass MALDI-MS^[4, 7, 10, 28] affords the pentamer subunit signal at $m/z = 97,600$ (theoretical MW = 88,420) as the dominant peak (Figure 1a, blue trace). The mass difference between the theoretical and the observed molecular weight of the pentamer subunit can be attributed to glutaraldehyde molecules that stabilize the pentamer.^[29] The good signal-to-noise ratio suggests that there is an appreciable fraction of pentamers present in the solution phase equilibrium between intact capsid and pentameric subunits. Although the small peak at $m/z = 195,100$ in Figure 1a (blue trace) could theoretically be attributed to an AaLS-13 decamer, it is more likely a result of nonspecific clustering, which typically occurs in the MALDI plume.^[30] We did not observe any signals from specific higher oligomeric states, nor from multiply charged ions corresponding to the entire capsid (see Figure 1a, insert). Since multiply charged ions can form in MALDI-MS of compounds with

very high molecular weight, we would expect to see signals of at least some oligomers in the mass range below 1.5 MDa if they were present at appreciable abundance; 1.5 MDa is the current limit of our MALDI instrument, which is essentially dictated by the instrument software. We interpret the absence of pentamer-dimers, trimers... (= 10mers, 15mers) and other higher oligomers to be due to slow crosslinking kinetics (crosslinking over night), which is exceeded by the assembly kinetics of the entire capsid.

In the following, we will demonstrate through a series of measurements that the exclusive presence of pentamer subunits in the MALDI spectra is not an analytical artifact, and more importantly, that the pentamers are associated with the structure of the intact capsid. To exclude effects from the cross-linking chemistry, we additionally applied native ESI-MS. Using native-ESI MS, the peaks observed in the high m/z range were also exclusively attributed to different charge states of pentamer subunits of the AaLS-13 capsid. In Figure 1b, the +19 and +18 ions of the AaLS-13 pentamer subunit dominate the spectrum. These results also suggest that the subunit composition is not affected by the transfer of the capsid into the gas phase, neither in ESI- nor in MALDI-based measurements. Our results, obtained with the help of native ESI-MS and MALDI-MS thus confirm the organization of AaLS-13 monomers into thermodynamically stable pentamer subunits, which form the building blocks of the intact capsid. Notably, hexamers, found in typical icosahedral structures^[24], are absent. This is in agreement with recent results obtained by cryo-EM, which show that the AaLS-13 capsid is composed of 72 pentamer subunits.^[25]

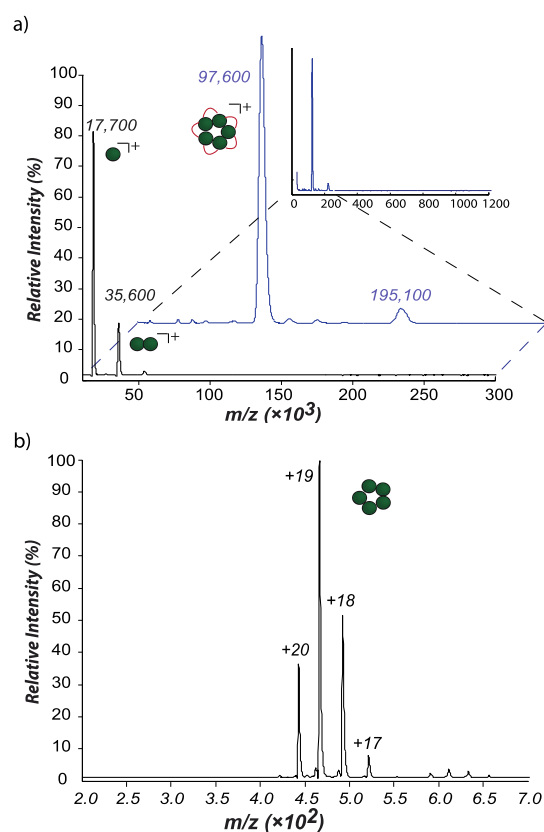


Figure 1. a) High-mass MALDI mass spectra of AaLS-13 before (black trace) and after cross-linking with glutaraldehyde (GA) 1% (blue trace) using sinapic acid (SA) (0.1% TFA). The insert shows a zoom-out spectrum showing that no other high molecular weight species were observed. b) Native ESI mass spectra of AaLS-13 in ammonium acetate (150 mM, pH = 8.0) in positive ion mode. The differently charged ion species were attributed to pentamer subunits.

Understanding the encapsulation of GFP(+36) by AaLS-13 capsids. We further investigated the capsid's properties as a protein encapsulation system. In particular, we were interested in the possibility to characterize the interaction between GFP(+36) and transient assembly intermediates using cross-linking MALDI-MS. It is known that up to ~ 90 GFP(+36) molecules (corresponding to ~ 1 GFP(+36) per 4 monomer units) can be encapsulated [15]. When mixing supercharged GFP(+36) cargo with AaLS-13 in a 1:4 molar ratio (GFP(+36):AaLS-13 monomer) in the absence of cross-linker, we observed MALDI-MS signals corresponding to both proteins (see Figure 2a black trace). The peak at $m/z = 17,700$ was identified as the monomer of AaLS-13, whereas the peak at $m/z = 28,500$ was attributed to supercharged GFP(+36) (theoretical $m/z = 28,651$). The peaks with minor intensities observed at $m/z = 56,900$ and $m/z = 85,950$ are due to non-specific clustering, which was mentioned above and is common in MALDI-MS.

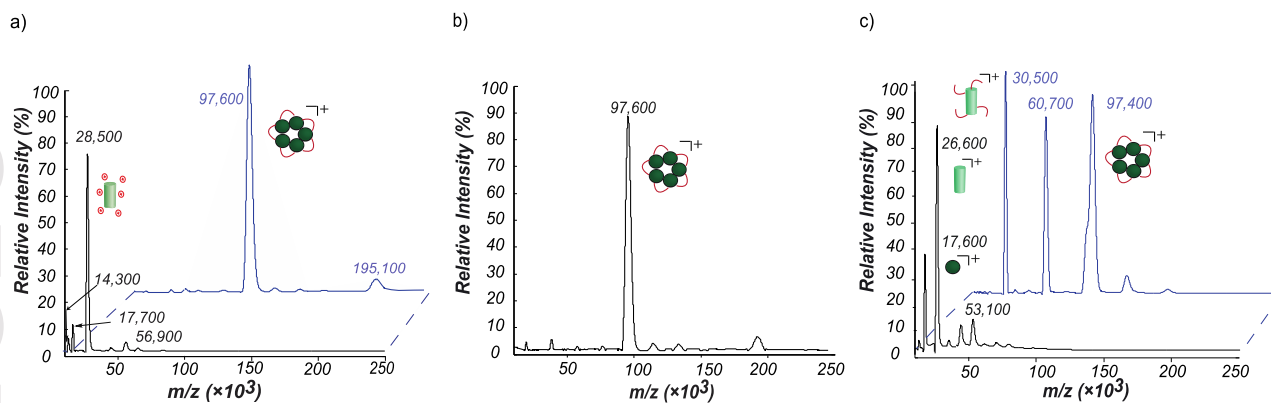


Figure 2. (a) High-mass MALDI mass spectra of AaLS-13 and supercharged GFP(+36) mixed at a monomer:GFP(+36) molar ratio of 4: 1 (v/v) before (black trace) and after (blue trace) cross-linking (1 % GA in SA (+0.1 % TFA) in positive ion mode). (b) After being independently cross-linked, GFP(+36) and AaLS-13 were mixed together. (c) AaLS-13 mixed with wild type GFP (w.t.) before (black) and after cross-linking (blue).

The addition of GA (see Figure 2a blue trace) leads to the detection of a peak at $m/z = 97,600$ representing the pentamer subunit (which is virtually identical to the result observed in the previous section, Figure 1a). At the same time, the previously dominant GFP(+36) signal disappeared after cross-linking. Interestingly, we observed no signals corresponding to formation of cross-links between GFP(+36) and either monomer or pentamer subunits of AaLS-13. Poor cross-linking efficiency is a possible explanation for the absence of signals corresponding to heterocomplexes in the MALDI mass spectra. Although it is now known that capsid loading is extremely rapid^[26] we originally suspected a slow encapsulation of GFP(+36) into AaLS-13 capsids, perhaps due to a sluggish association of GFP(+36) with pentamer units, for example due to presence of inactivated cross-linker that fails to stabilize heterocomplexes. To check this, we added cross-linker-free capsid to GFP(+36) that had already been mixed with GA (10 mins.), and subsequently added more GA to the mixture to ensure cross-linking of subunits (see Figure 2b). However, again neither GFP(+36) signal nor the formation of any heterocomplex was observed. Thus, the absence of GFP(+36) cross-linked with the pentamer subunit does not originate from an inactive cross-linker.

An alternative explanation is the well-known effect of ion suppression in mass spectrometry, which might cause the signal of GFP(+36) to vanish. Therefore, we replaced supercharged GFP(+36) in the previous experiment with wild-type GFP (w.t. GFP), which does not possess the same highly positively charged surface as its genetically modified counterpart and is not encapsulated by the capsid. Thus, we mixed w.t. GFP with AaLS-13 and subsequently performed chemical cross-linking.

The results are shown in Figure 2c. Before the addition of the cross-linking agent, we observed a dominant peak at $m/z = 26,600$, which corresponds to the monomer of w.t. GFP. The other peaks with minor intensity arise from non-specific oligomer formation. After cross-linking, we could clearly identify the presence of both the AaLS-13 pentamer subunit at $m/z = 97,400$ and the monomer of w.t. GFP at $m/z = 30,500$. The peak at $m/z = 60,700$ was attributed to the dimer of w.t. GFP as previously described in the literature.^[31] Neutralization by interaction with oppositely charged matrix can be ruled out, since matrix and GFP(+36) alone allow successful detection of GFP. The experiments were carried out in stoichiometric deficiency of GFP(+36) compared to AaLS-13 monomer (AaLS-13monomer:GFP(+36) 4:1). Exceeding the maximal loading capacity results in aggregation^[26]. Alternatively, the absence of GFP(+36) signal could be due to formation of insoluble GFP(+36) aggregates. However, this would be incompatible with the observation of a dominant signal of GFP(+36) when mixed with capsid prior to crosslinking. After incubating GFP(+36) with the cross-linker in the absence of the capsid, the signal of GFP(+36) shifted to higher m/z . This is explained by reaction of solvent exposed amino acids of GFP(+36) with GA (see SI1). Moreover, The signal of GFP(w.t.), which has a similar amino acid sequence and thus similar solvent exposed groups as GFP(+36) was successfully detected when mixed with AaLS-13 capsid after cross-linking. Thus, we interpret the absence of supercharged GFP(+36) after cross-linking as an indication for GFP(+36) being efficiently encapsulated. Unfortunately, the molecular weight of the complex of the capsid with supercharged GFP(+36) lies well beyond the 1.5 MDa limit of our instrument, thus preventing us from detecting the entire complex or any mass shift that would arise from encapsulation of supercharged GFP(+36). Our interpretation of GFP(+36) incorporation into the capsid is thus based on an indirect observation, namely that the encapsulation efficiently removes GFP(+36) from the solution, and that crosslinking with GA stabilizes the capsid plus its encapsulated cargo, which leads to the complete disappearance of GFP(+36) from the MALDI mass spectrum. Only some pentamer subunits remain, which are observed.

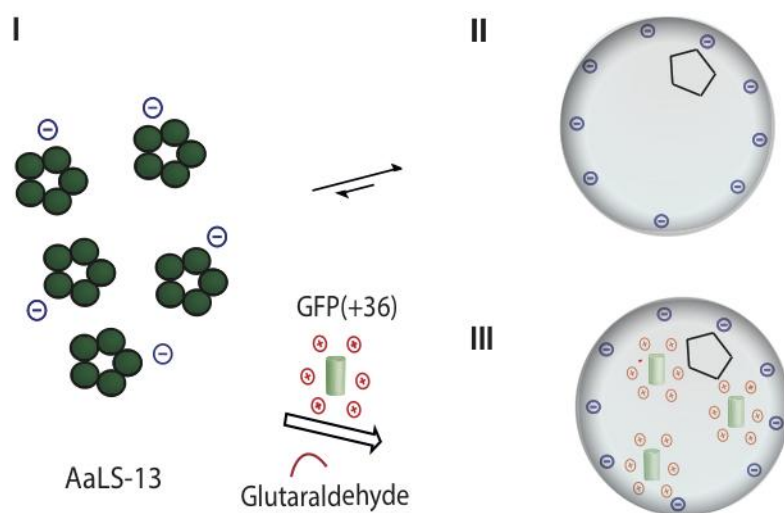


Figure 3. Schematic outline of the capsid formation process via self-assembly process. I) AaLS-13 monomers assemble into thermodynamically stable subunits. II) The equilibrium between the subunits and the capsid is shifted to the formation of the entire capsid. III) The encapsulation of supercharged GFP(+36) is promoted by electrostatic attraction between the highly positively charged GFP(+36) and the negatively charged AaLS-13.

Figure 3 shows a schematic representation of capsid formation as well as GFP(+36) incorporation into the AaLS-13 capsid. In the absence of supercharged GFP(+36) the equilibrium between pentameric subunits and the self-assembled capsid favors intact cage formation (see Figure 3 I-II). Upon addition of GFP(+36), assembled capsids efficiently encapsulate guest (Figure 3-III). Zschoche *et al.* have shown the encapsulation process to be very rapid ($< \tau_{1/2} \sim 50$ ms; ionic strength of the buffer I = 550 mM).^[26] This efficient encapsulation of guest by the capsid simply removes GFP(+36) from the solution, and it would neither be visible alone nor available to form heterocomplexes.

CryoEM has evolved into a very high resolution (down to $\leq 2\text{\AA}$ in the best case) and thus very information-rich methodology, but requires careful consideration of several parameters, including controlled sample preparation for structural homogeneity, accurate determination of imaging parameters in order to correct image distortions, as well as efficient refinement of modeling tools for construction of atomic models for functional interpretation.^[32] Optimizing these parameters is time-consuming (weeks to sometimes months). Compared to cryoEM, in-situ crosslinking followed by MALDI-MS is a rather straightforward technique, which after cross-linker screening and optimization yields results on the complex connectivity within a few days only. Therefore, MALDI-MS could be used as an alternative analytical tool to obtain initial insight into subunit composition of capsid complexes that are often challenging and time-consuming to investigate with standard techniques.

CONCLUSIONS

We demonstrated that *in-situ* cross-linking with GA followed by MALDI-MS could successfully map the subunit composition of an engineered AaLS-13 capsid. For this relatively large protein capsid, we were able to detect subunits of the engineered variant AaLS-13 with the help of two complementary methods, native ESI and MALDI-MS. Only pentamer subunits were observed for AaLS-13, which is in agreement with the structure recently obtained by cryo-EM. We did not observe higher cross-linking products beyond pentamer subunits, nor multiply charged entirely cross-linked capsids. This is very likely due to the detection limit of our instrument (1.5 MDa). This method could be further expanded for subunit characterization of other protein containers provided that reactive amino acid side chains are solvent accessible and sufficiently close for cross-linking.

We also probed whether cross-linking high-mass MALDI-MS can be used to gain insight into the encapsulation of supercharged GFP(+36) by AaLS-13. After mixing GFP(+36) with the capsid at the maximal loading capacity (AaLS-13monomer:GFP(+36) 4:1), the dominant GFP(+36) signal in the mass spectrum vanished after the addition of cross-linker (GA). The presence of GA stabilizes the intact capsid, which can efficiently encapsulate GFP(+36), and remove it from the solution.

Unfortunately, the molecular weight of the entire host-guest complex lies beyond the limit of our instrument, thus preventing us from detecting the complex loaded with supercharged GFP(+36).

EXPERIMENTAL SECTION

Materials and Methods

Materials. Acetonitrile (>99.0% for LC-MS), ammonium acetate (> 99.0% for LC-MS), formic acid (98%) were obtained from Fluka-Chemie (Buchs, Switzerland). Sinapic acid (SA) matrix, glutaraldehyde (50 wt % in H₂O), trifluoroacetic acid (TFA, > 99% for HPLC), glyceraldehyde-3-phosphate-dehydrogenase (GAPDH) and isopropanol (> 99.8% for HPLC) were purchased from Sigma-Aldrich Chemie GmbH (Buchs, Switzerland). Tris-(2-carboxyethyl)phosphine (TCEP) hydrochloride was purchased from ABCR Chemicals (Karlsruhe, Germany). The engineered variant AaLS-13 was expressed and purified as described before.^[15]

Buffer Exchange. Amicon ultra centrifugal filter columns with a 10 kDa MW cut-off (Millipore Ltd., Tullagreen Carrigtwohill, Ireland) were used to perform buffer exchange of the protein samples for native mass spectrometry. Prior to loading the sample, the ultrafiltration columns were loaded with

500 μ L of buffer (ammonium acetate 150 mM, pH = 8.0) and centrifuged to remove impurities from the membrane. A refrigerated microcentrifuge MicroCL17R (Thermo Scientific, Madison, WI, USA) was used, which was operated at 4 °C and 14000 rcf. After washing the membrane, 50 μ L of protein solution were loaded on the column and centrifuged several times until buffer exchange was achieved (> 99.99%). For MALDI cross-linking experiments, 50 mM of sodium phosphate buffer containing 200 mM NaCl and 5mM EDTA (pH = 8.0) was used for the protein capsids as well as PBS buffer containing 2 M NaCl for the supercharged GFP protein. For native ESI-MS experiments, ammonium acetate buffer (150 mM, pH = 8.0) was used.

Determination of the Protein Concentration. The concentration of the protein samples was determined by measuring the UV absorbance at 280nm with a Genesys 10S UV/VIS spectrophotometer (Thermo Scientific, Madison, WI, USA) utilizing plastic UV cuvettes (UVette, Vaudax-Eppendorf AG, Schönenbuch/Basel, Switzerland). The same buffer was used as a blank. The monomer concentration of AaLS-13 was calculated by utilizing the Lambert-Beer law (extinction coefficient $\epsilon_{280} = 14,105 \text{ cm}^{-1}\text{M}^{-1}$).

Chemical Cross-Linking. Because MALDI-MS often disrupts weak noncovalent interactions, chemical cross-linking was used to stabilize capsids, subunits and oligomers on the way to the fully formed capsid^[4]. Chemical cross-linking of AaLS-13 in buffer solution was performed according to the protocol of Mädler *et al.*^[28, 33]. The protein solution was diluted to a final pentamer concentration of 20 mM. The capsid protein was mixed with a 10% aqueous glutaraldehyde (GA) solution in a ratio of 10/1 (v/v) and allowed to react overnight at room temperature. For AaLS-13, reduction of disulfide bond formation was performed by the addition of a tris-(2-carboxyethyl)phosphine (TCEP) solution (500 μ M) to the protein solution in a 1:10 (v/v) ratio.

MALDI-MS Analysis. Sinapic acid (10mg/ml) dissolved in water/acetonitrile/TFA (49.95/49.95/0.1 (v/v/v)) was used as a matrix. The protein sample was mixed directly with the matrix in a 1/1 (v/v) ratio. 1 μ L of the mixture was pipetted onto a stainless steel plate and was left to dry at ambient conditions to allow crystallization. A commercial MALDI time-of flight (TOF)/TOF mass spectrometer (4800 Plus, AB Sciex, Darmstadt, Germany) equipped with a high-mass ion conversion detector (HM2 Tuvo, CovalX AG, Zurich, Switzerland) was used. All experiments were carried out in positive ion mode with standard settings. The ionization was performed by a Nd:YAG laser (355 nm). A GAPDH

solution (40 μ M, in PBS) was used for external calibration. Typically, each mass spectrum represents an average of 1000 automatically recorded laser shots acquired at random spot positions. After recording, mass spectra were exported (ASCII format) using the instrument software (4000 Series Explorer V.3.5.3), for further data processing. The MALDI instrument currently has an upper limit of 1.5 MDa, essentially restricted by the instrument software^[11]. As described previously, a concatenated form of maltose binding protein (MBP)^[34] was used as an internal standard for quantification of the pentamer signal.

Native Electrospray Ionization Mass Spectrometry. Native ESI-mass spectrometry was carried out on a commercial hybrid quadrupole time-of-flight mass spectrometer (Q-TOF Ultima API, Micromass, Manchester, UK), which is equipped with a 8k quadrupole and a modified high-pressure collision cell. All experiments were carried out in positive ion mode. Typically, 3-5 μ L of sample were loaded into 1 μ m Au/Pd coated glass needles (Thermo Scientific, Madison, WI, USA). For electrospray generation, a commercial nano-ESI source was used at ambient temperature by applying 1.9-2.3 kV. The backing pressure was set to 2.0 bar to assist sample flow. For gentle transmission of the ions formed in the spray region operated at atmospheric pressure to vacuum, the pressure inside the first pumping compartment was increased to 3.5 -4.0 mbar. The settings of the cone voltage, RF1, offset 1 and the collision energy were optimized to obtain efficient ion transfer, good signal intensity and resolution. The quadrupole transmission range was adjusted for the desired m/z range. The mass spectra were recorded in a m/z window of 50-8000 with a scan time of 2 s and an interscan delay of 0.1 s. Each native ESI mass spectrum is the average of 50 individual scans. Due to a limitation of the transmission of our current 8k quadrupole, it is not possible to detect the intact capsid.

Mass spectra were recorded using the MassLynx 4.0 software (Waters, Manchester, UK). All mass spectra were baseline corrected, normalized and smoothed using MATLAB_R2014a. For calibration, CsI clusters (10 mg/ml) dissolved in 50 % (v) isopropanol were used. The recorded spectra were averaged (500 scans), smoothed with a moving algorithm (width of 3 steps) and centroid spectra were generated at 80 % peak height. The mass axis was calibrated after polynomial fitting.

ASSOCIATED CONTENT

Supplementary Material

Additional information as noted in the text. This material is available free of charge via the Internet at <http://pubs.acs.org>.

AUTHOR CONTRIBUTION STATEMENT

Project design, data analysis and writing of the manuscript by K.R. Proteins were expressed and purified by R.F. Correction of the manuscript by D.H. and R.Z.

AUTHOR INFORMATION

Corresponding Author

* Telephone +41 44 632 43 76; Fax +41 44 632 12 92; email: zenobi@org.chem.ethz.ch

Notes

The authors declare no competing financial interest.

ACKNOWLEDGMENT

The Swiss National Science Foundation (SNF, 200020_159929) as well as the European Research Council (ERC-AdG-2012-321245) supported this research.

REFERENCES

- [1] J. Snijder, R. J. Rose, D. Veessler, J. E. Johnson, A. J. Heck, 'Studying 18 MDa virus assemblies with native mass spectrometry', *Angew. Chem. Int. Ed.* **2013**, *52*, 4020-4023.
- [2] C. Uetrecht, A. J. Heck, 'Modern biomolecular mass spectrometry and its role in studying virus structure, dynamics, and assembly', *Angew. Chem. Int. Ed.* **2011**, *50*, 8248-8262.
- [3] G. Bolbach, 'Matrix-assisted laser desorption/ionization analysis of non-covalent complexes: fundamentals and applications', *Curr. Pharm. Des.* **2005**, *11*, 2535-2557.
- [4] F. Chen, B. Gulbakan, S. Weidmann, S. R. Fagerer, A. J. Ibanez, R. Zenobi, 'Applying mass spectrometry to study non-covalent biomolecule complexes', *Mass Spectrom. Rev.* **2016**, *35*, 48-70.
- [5] F. Chen, S. Gerber, K. Heuser, V. M. Korkhov, C. Lizak, S. Mireku, K. P. Locher, R. Zenobi, 'High-Mass Matrix-Assisted Laser Desorption Ionization-Mass Spectrometry of Integral Membrane Proteins and Their Complexes', *Anal. Chem.* **2013**, *85*, 3483-3488.

- [6] P. Lossl, J. Snijder, A. J. Heck, 'Boundaries of mass resolution in native mass spectrometry', *J. Am. Soc. Mass. Spectrom.* **2014**, *25*, 906-917.
- [7] J. Snijder, M. van de Waterbeemd, E. Damoc, E. Denisov, D. Grinfeld, A. Bennett, M. Agbandje-McKenna, A. Makarov, A. J. Heck, 'Defining the stoichiometry and cargo load of viral and bacterial nanoparticles by Orbitrap mass spectrometry', *J. Am. Chem. Soc.* **2014**, *136*, 7295-7299.
- [8] E. E. Pierson, D. Z. Keifer, A. Asokan, M. F. Jarrold, 'Resolving Adeno-Associated Viral Particle Diversity With Charge Detection Mass Spectrometry', *Anal. Chem.* **2016**, *88*, 6718-6725.
- [9] E. E. Pierson, D. Z. Keifer, A. A. Kukreja, J. C. Wang, A. Zlotnick, M. F. Jarrold, 'Charge Detection Mass Spectrometry Identifies Preferred Non-Icosahedral Polymorphs in the Self-Assembly of Woodchuck Hepatitis Virus Capsids', *J. Mol. Biol.* **2016**, *428*, 292-300; D. Z. Keifer, T. Motwani, C. M. Teschke, M. F. Jarrold, 'Measurement of the accurate mass of a 50 MDa infectious virus', *Rapid Commun. Mass Spectrom.* **2016**, *30*, 1957-1962; D. Z. Keifer, T. Motwani, C. M. Teschke, M. F. Jarrold, 'Acquiring Structural Information on Virus Particles with Charge Detection Mass Spectrometry', *J. Am. Soc. Mass. Spectrom.* **2016**, *27*, 1028-1036; J. Snijder, J. M. Schuller, A. Wiegard, P. Lossl, N. Schmelling, I. M. Axmann, J. M. Plitzko, F. Forster, A. J. Heck, 'Structures of the cyanobacterial circadian oscillator frozen in a fully assembled state', *Science* **2017**, *355*, 1181-1184; M. van de Waterbeemd, J. Snijder, I. B. Tsvetkova, B. G. Dragnea, J. J. Cornelissen, A. J. Heck, 'Examining the Heterogeneous Genome Content of Multipartite Viruses BMV and CCMV by Native Mass Spectrometry', *J. Am. Soc. Mass. Spectrom.* **2016**, *27*, 1000-1009.
- [10] M. A. Tito, K. Tars, K. Valegard, J. Hajdu, C. V. Robinson, 'Electrospray time-of-flight mass spectrometry of the intact MS2 virus capsid', *J. Am. Chem. Soc.* **2000**, *122*, 3550-3551.
- [11] C. Uetrecht, C. Versluis, N. R. Watts, W. H. Roos, G. J. L. Wuite, P. T. Wingfield, A. C. Steven, A. J. R. Heck, 'High-resolution mass spectrometry of viral assemblies: Molecular composition and stability of dimorphic hepatitis B virus capsids', *Proc. Natl. Acad. Sci. USA* **2008**, *105*, 9216-9220.
- [12] L. D. Plath, A. Ozdemir, A. A. Aksenov, M. E. Bier, 'Determination of iron content and dispersity of intact ferritin by superconducting tunnel junction cryodetection mass spectrometry', *Anal. Chem.* **2015**, *87*, 8985-8993.
- [13] S. A. Bode, I. J. Minten, R. J. Nolte, J. J. Cornelissen, 'Reactions inside nanoscale protein cages', *Nanoscale* **2011**, *3*, 2376-2389; T. Beck, S. Tetter, M. Kunzle, D. Hilvert, 'Construction of Matryoshka-type structures from supercharged protein nanocages', *Angew. Chem. Int. Ed.* **2015**, *54*, 937-940; A. de la Escosura, R. J. M. Nolte, J. J. L. M. Cornelissen, 'Viruses and protein cages as nanocontainers and nanoreactors', *J. Mater. Chem.* **2009**, *19*, 2274-2278.
- [14] F. P. Seebeck, K. J. Woycechowsky, W. Zhuang, J. P. Rabe, D. Hilvert, 'A simple tagging system for protein encapsulation', *J. Am. Chem. Soc.* **2006**, *128*, 4516-4517.
- [15] Y. Azuma, R. Zschoche, M. Tinzl, D. Hilvert, 'Quantitative Packaging of Active Enzymes into a Protein Cage', *Angew. Chem. Int. Ed.* **2016**, *55*, 1531-1534.
- [16] N. M. Molino, S. W. Wang, 'Caged protein nanoparticles for drug delivery', *Curr. Opin. Biotechnol.* **2014**, *28*, 75-82.
- [17] I. Yildiz, K. L. Lee, K. Chen, S. Shukla, N. F. Steinmetz, 'Infusion of imaging and therapeutic molecules into the plant virus-based carrier cowpea mosaic virus: Cargo-loading and delivery', *J. Controlled Release* **2013**, *172*, 568-578.

- [18] X. T. Ji, L. Huang, H. Q. Huang, 'Construction of nanometer cisplatin core-ferritin (NCC-F) and proteomic analysis of gastric cancer cell apoptosis induced with cisplatin released from the NCC-F', *J Proteomics* **2012**, *75*, 3145-3157; Z. P. Zhen, W. Tang, H. M. Chen, X. Lin, T. Todd, G. Wang, T. Cowger, X. Y. Chen, J. Xie, 'RGD-Modified Apoferritin Nanoparticles for Efficient Drug Delivery to Tumors', *Acs Nano* **2013**, *7*, 4830-4837; I. Yamashita, K. Iwahori, S. Kumagai, 'Ferritin in the field of nanodevices', *Bba-Gen Subjects* **2010**, *1800*, 846-857; D. D. He, J. Marles-Wright, 'Ferritin family proteins and their use in bionanotechnology', *New Biotechnol* **2015**, *32*, 651-657.
- [19] T. J. Todd, Z. Zhen, J. Xie, 'Ferritin nanocages: great potential as clinically translatable drug delivery vehicles?', *Nanomedicine* **2013**, *8*, 1555-1557.
- [20] T. O. Yeates, C. A. Kerfeld, S. Heinhorst, G. C. Cannon, J. M. Shively, 'Protein-based organelles in bacteria: carboxysomes and related microcompartments', *Nat. Rev. Microbiol.* **2008**, *6*, 681-691; C. V. Iancu, H. J. Ding, D. M. Morris, D. P. Dias, A. D. Gonzales, A. Martino, G. J. Jensen, 'The structure of isolated *Synechococcus* strain WH8102 carboxysomes as revealed by electron cryotomography', *J. Mol. Biol.* **2007**, *372*, 764-773; S. Tanaka, C. A. Kerfeld, M. R. Sawaya, F. Cai, S. Heinhorst, G. C. Cannon, T. O. Yeates, 'Atomic-level models of the bacterial carboxysome shell', *Science* **2008**, *319*, 1083-1086; S. Tanaka, M. R. Sawaya, M. Phillips, T. O. Yeates, 'Insights from multiple structures of the shell proteins from the beta-carboxysome', *Protein Sci.* **2009**, *18*, 108-120.
- [21] B. Worsdorfer, K. J. Woycechowsky, D. Hilvert, 'Directed evolution of a protein container', *Science* **2011**, *331*, 589-592.
- [22] M. S. Lawrence, K. J. Phillips, D. R. Liu, 'Supercharging proteins can impart unusual resilience', *J. Am. Chem. Soc.* **2007**, *129*, 10110-10112.
- [23] R. Frey, S. Mantri, M. Rocca, D. Hilvert, 'Bottom-up Construction of a Primordial Carboxysome Mimic', *J. Am. Chem. Soc.* **2016**, *138*, 10072-10075.
- [24] B. Worsdorfer, Z. Pianowski, D. Hilvert, 'Efficient in vitro encapsulation of protein cargo by an engineered protein container', *J. Am. Chem. Soc.* **2012**, *134*, 909-911.
- [25] E. Sasaki, D. Bohringer, M. van de Waterbeemd, M. Leibundgut, R. Zschoche, A. J. Heck, N. Ban, D. Hilvert, 'Structure and assembly of scalable porous protein cages', *Nat. Commun.* **2017**, *8*, 14663.
- [26] R. Zschoche, D. Hilvert, 'Diffusion-Limited Cargo Loading of an Engineered Protein Container', *J. Am. Chem. Soc.* **2015**, *137*, 16121-16132.
- [27] I. Migneault, C. Dartiguenave, M. J. Bertrand, K. C. Waldron, 'Glutaraldehyde: behavior in aqueous solution, reaction with proteins, and application to enzyme crosslinking', *Biotechniques* **2004**, *37*, 790-800.
- [28] C. Bich, S. Maedler, K. Chiesa, F. DeGiacomo, N. Bogliotti, R. Zenobi, 'Reactivity and Applications of New Amine Reactive Cross-Linkers for Mass Spectrometric Detection of Protein-Protein Complexes', *Anal. Chem.* **2010**, *82*, 172-179.
- [29] F. Chen, S. Nielsen, R. Zenobi, 'Understanding chemical reactivity for homo- and heterobifunctional protein cross-linking agents', *J. Mass Spectrom.* **2013**, *48*, 807-812; F. Chen, S. Madler, S. Weidmann, R. Zenobi, 'MALDI-MS detection of noncovalent interactions of single stranded DNA with *Escherichia coli* single-stranded DNA-binding protein', *J. Mass Spectrom.* **2012**, *47*, 560-566.

- [30] V. Livadaris, J. C. Blais, J. C. Tabet, 'Formation of non-specific protein cluster ions in matrix-assisted laser desorption/ionization: abundances and dynamical aspects', *Eur J Mass Spectrom* **2000**, *6*, 409-413.
- [31] R. Y. Tsien, 'The green fluorescent protein', *Annu. Rev. Biochem* **1998**, *67*, 509-544.
- [32] Z. H. Zhou, 'Atomic Resolution Cryo Electron Microscopy of Macromolecular Complexes', *Adv Protein Chem Str* **2011**, *82*, 1-35.
- [33] S. Madler, C. Bich, D. Touboul, R. Zenobi, 'Chemical cross-linking with NHS esters: a systematic study on amino acid reactivities', *J. Mass Spectrom.* **2009**, *44*, 694-706.
- [34] S. Weidmann, K. Barylyuk, N. Nespovityaya, S. Madler, R. Zenobi, 'A New, Modular Mass Calibrant for High-Mass MALDI-MS', *Anal. Chem.* **2013**, *85*, 3425-3432.